ELSEVIER

Journal of Nuclear Materials 290–293 (2001) 276–280

journal of nuclear materials

www.elsevier.nl/locate/jnucmat

Comparison of impurity production, recycling and power deposition on carbon and tungsten limiters in TEXTOR-94

A. Huber [a,*], V. Philipps [a], A. Pospieszczyk [a], A. Kirschner [a], M. Lehnen [a], T. Ohgo [b], K. Ohya [c], M. Rubel [d], B. Schweer [a], J. von Seggern [a], G. Sergienko [e], T. Tanabe [f], M. Wada [g]

[a] *Institut für Plasmaphysik, Forschungszentrum Jülich GmbH, EURATOM Association, Trilateral Euregio Cluster, D-52425 Jülich, Germany*

[b] *Department of Physics, Fukuoka University of Education, Fukuoka, Japan*

[c] *Department of Electrical Engineering and Electronics, University of Tokushima, Tokushima, Japan*

[d] *Royal Institute of Technology, Alfven Laboratory, S-10044 Stockholm, Sweden*

[e] *Institute of High Temperatures, Russian Academy of Sciences, Moscow, Russian Federation*

[f] *Center for Integrated Research in Science and Engineering, Nagoya, Japan*

[g] *Department of Electronics, Doshisha University, Kyotanabe, Japan*

Abstract

Impurity production, hydrogen recycling and power deposition on carbon and tungsten limiters have been investigated in TEXTOR-94 using a C–W twin test limiter. Considerable differences have been observed on W and C surfaces, which can be explained by the different particle and energy reflection coefficients of hydrogen on these surfaces. The measurements show in addition that the majority of the carbon release is from recycled carbon and that only a small part (below 10%) is due to net-erosion from the bulk carbon material. The heat deposition on C and W sides differs under the same plasma conditions significantly and is typically about 30% larger on the carbon surface. The behaviour of the impurity production, recycling and power deposition for various discharge conditions is presented.

Keywords: Carbon; Carbon erosion; Impurity; Power deposition; Recycling; Spectroscopy; Tungsten; TEXTOR 94

1. Introduction

Carbon and tungsten are considered to be favourable candidates for low- and high-Z plasma facing materials in fusion devices [1]. Carbon is a material which is best suited to withstand transient heat pulses and off-normal events since it does not melt and preserves its shape. It suffers, however, from large erosion yields which leads to the formation of carbon deposits which can store the majority of the long-term tritium inventory. Tungsten has the advantage of very low erosion yields. But its concentration in the plasma core must be kept below a critical level of about 10^{-5} in order to prevent strong radiation losses. When overloaded it can also melt. It is important to determine the interaction of the plasma with both materials in detail. In order to directly compare the impurity production and recycling at carbon and tungsten surfaces in a tokamak, a C–W twin test limiter, one half made of tungsten and the other half made of carbon, was inserted into the edge plasma of TEXTOR-94. The release of impurities (W, C, O) from different surfaces (C and W) is examined spectroscopically and power deposition is measured by infrared thermography. By 180° rotation of the limiter identical conditions with respect to the plasma parameters and observation geometry could be provided.

* Corresponding author. Tel. +49-2461 2631; fax: +49-2461 2660.

E-mail address: a.huber@fz-juelich.de (A. Huber).

0022-3115/01/$ - see front matter
PII: S0022-3115(00)00629-2

2. Experimental set-up

The experiments have been performed in the tokamak TEXTOR-94 with a major radius $R = 1.75$ m and a minor radius $a = 0.46$ m. TEXTOR-94 was operated at a toroidal magnetic field of $B_T = 2.25$ T and plasma current of $I_p = 350$ kA. The line-averaged central electron density was varied between $\bar{n}_e = 2 \times 10^{19}$ m^{-3} and $\bar{n}_e = 6 \times 10^{19}$ m^{-3}. Additional heating was provided by a neutral beam injector (NBI) injecting tangentially in the co-direction of the current with a power of 1.3–1.5 MW.

A C–W twin test limiter with dimensions of 12 cm × 8 cm and a spherical shape with a radius of 7 cm was inserted from the top of the torus into the edge plasma through a limiter-lock [2] to the position of the last closed flux surface (LCFS). The limiter can be rotated in-between shots, making it possible to face the C- or the W-side of the twin limiter either to the ion drift or the electron drift direction, thus allowing to perform investigations of both sides under identical plasma conditions.

The radial distributions of spectral line intensities of emissions from ions and neutrals in front of the test limiter were measured by an image intensified CCD-camera coupled to a spectrometer (Ebert type, $f = 0.5$ m), the entrance slit of which was focussed at a toroidal position 20 mm from the centre at the ion drift side. The 2D intensity distribution of impurity line emissions (W, C) was observed by an additional CCD-camera coupled to interference filters with a bandwidth of 1.5 nm for the respective impurity line radiation. The power deposition on the limiter surface was measured by a pyrometer and a third CCD-camera with an infrared edge filter (transmission wavelength from 850 to 1100 nm). Additionally the bulk temperature of each limiter side was monitored with thermocouples 7 mm behind the surface near the location of the highest power load. Edge electron temperature and density profiles were measured at the equatorial plane by means of He-beam diagnostics [3].

3. Results and discussion

3.1. Impurity production

Fig. 1 shows the typical emission spectra in front of the carbon and the tungsten section of the twin limiter in the wavelength range between 409 and 436 nm. These spectra are recorded in discharges with additional NBI-heating with $P_{NBI} = 1.3$ MW and a line-averaged electron density of 3×10^{19} m^{-3}. The spectrometer allows the simultaneous observation of several emission lines, e.g., chromium, boron, carbon, tungsten, oxygen, hydrogen and molecular CD-bands. When the limiter

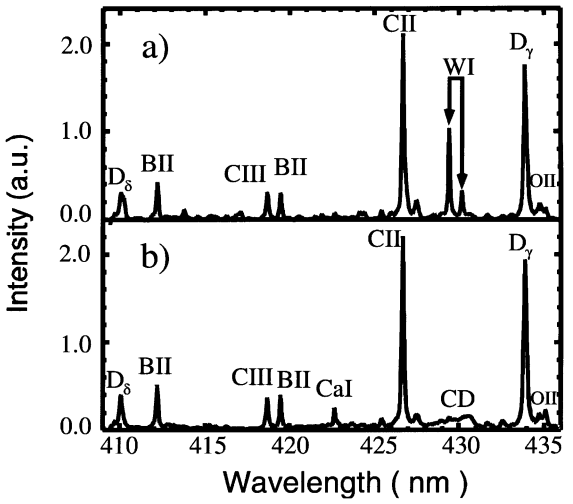

Fig. 1. Typical spectra of plasma in front of tungsten (a) and carbon (b) limiters.

material was changed from graphite to tungsten, a strong emission of WI (429.5 nm) was observed, accompanied by a strong reduction in the emission band of the CD-radical (430.7 nm).

Fig. 2 shows the measured radial profiles of the CII light emission on both surfaces together with profiles calculated with the ERO-TEXTOR code [4]. The code calculations are based on the measured profiles of temperature and density, ionization cross-sections taken from Lotz [5] data and a constant chemical erosion yield for CD_4 of 3%. The effective sticking coefficients for the returning hydrocarbon species from the break up of methane have been set to $S_{ion} = 0.5$ and $S_{neutral} = 0$ [6]. The amount of carbon released in the form of hydrocarbons from the tungsten surface is small compared to a graphite surface (CD-emission in Fig. 1) and in the simulation for the tungsten side chemical erosion is, therefore, neglected. The fraction of the CII-emission which is attributed to reflected carbon is significantly larger at the W surface which leads to the broadening of the radial CII distribution on the W side. In addition, the penetration depth of the CII-emissions originating from hydrocarbons is shorter than that from physically sputtered carbon atoms which also contributes to the peaking of the radial distribution of CII-emission in front of the carbon limiter. Fig. 2 shows that the agreement between measured and calculated profiles is very good. The penetration depth of the CII-emission at the W-surface is about ≈15% larger than at the graphite surface.

The limiter heads were investigated post-mortem with ion beam analysis to determine the spatial distribution and quantity of species deposited on the limiter surface [7]. It was found that in the central region of the spherically shaped tungsten limiter, where the spectroscopy measurements have been performed, no significant

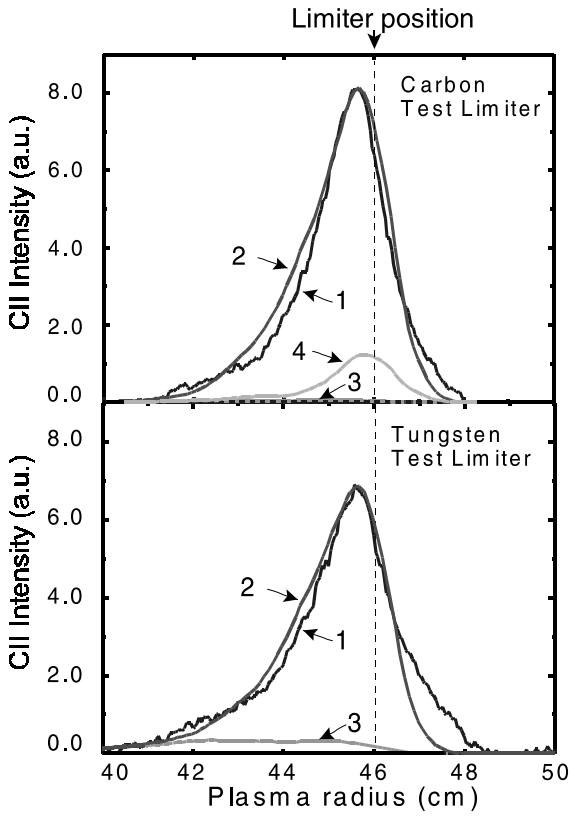

Fig. 2. Comparison of experimental (1) and simulated (2) CII-emission profiles in radial direction from carbon (top) and tungsten (bottom) limiters. The simulated profile has a contribution due to background reflected C particles (3), chemical (4) (only for C-limiter) and physical sputtering.

deposition of carbon (<1 monolayer) is found. However, deeper in the scrape-off layer (SOL) at the outer regions of the limiter, a region of carbon net deposition was detected.

The CII-emission in front of the tungsten limiter results thus from carbon, which is first implanted in the near-surface layer but is then immediately re-sputtered. Since no carbon layer is formed, the number of carbon sticking on these areas of net erosion is equal to the number of sputtered carbon neutrals. Thus, the measured C-flux at the W surface results only from the recycling of the carbon impurities flowing in the plasma edge, whereas the emission of the carbon at the C surface can originate from the recycled carbon impurities and from carbon eroded from the bulk of the graphite limiter. For the case shown in Fig. 2 ($\bar{n}_e = 3 \times 10^{19}$ m^{-3}, $P_{NBI} = 1.3$ MW), the calculated C-fluxes on the C and W sides of the limiter, normalized to the same D-flux, are 3.3% and 3.1%, respectively. We conclude that only the difference of 0.2% has to be attributed to carbon being eroded from the graphite material and representing the net-erosion. Thus, under these conditions the net-erosion is below 10% of the gross-erosion.

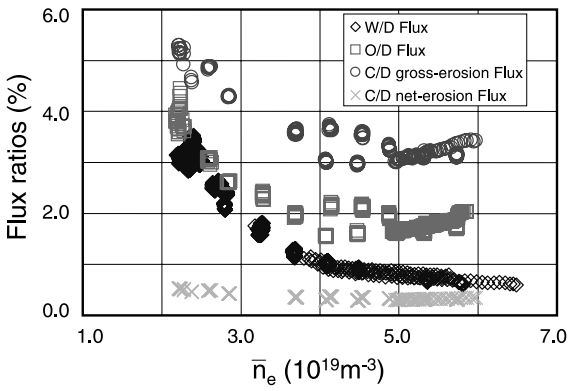

Fig. 3. Density dependence of the relative C/D and O/D fluxes emitted from the C-limiter and of the W/D flux from the W-limiter side. The net-erosion C/D flux was calculated under the assumption that net-erosion is about 10% of the gross-erosion.

Fig. 3 shows the relative carbon and oxygen fluxes emitted from the C-limiter. The measurements were made in a sequence of shots with additional NBI-heating of $P_{NBI} = 1.5$ MW. The C/D flux ratio is obtained from a CII line at 426.7 nm and D_γ using a ratio for the ionization to photon rates S/XB(CII):S/XB(D_γ) of 0.035. The O/D flux ratio is evaluated using a ratio of S/XB(OII $\lambda = 424.6$ nm):S/XB(D_γ) of 0.1. As it can be seen, the yields decrease with increasing line averaged electron densities: the C/D flux ratio decreases from 5% to 3% and the O/D flux from 4% to 2%, respectively. For expected $\bar{n}_e$, the local electron temperature varies between 90 and 30 eV and the local electron density varies between $n_e = 4 \times 10^{18}$ m^{-3} and $n_e = 1.6 \times 10^{19}$ m^{-3}. Fig. 3 also shows the flux ratio of W/D from the W-limiter evaluated from a neutral WI line emission at 495 nm. This line was cross calibrated with a WI line at 400.8 nm and it was found that I_{WI} (400.8 nm) = I_{WI} (429.5 nm). The ionization events/photon emission of the line at 400.8 nm is about 30 [8] in the temperature range of interest and a ratio of S/XB(WI = 400.8 nm; WI = 429.5 nm):S/XB(D_γ) of 0.03 has been used here. As can be seen, the W/D flux ratio decreases rather strongly with plasma density and decreasing edge electron temperature. At an electron density of $\bar{n}_e = 6.5 \times 10^{19}$ m^{-3} the W/D flux is only 0.5%. A more detailed analysis shows [2] that the majority of the tungsten is released by impurity sputtering rather than by deuterium impact. The figure also shows the carbon net-erosion using the value of 10% as evaluated above.

3.2. Recycling

Fig. 4 compares the radial distributions of the D_γ-emission from the tungsten and carbon sides. Although

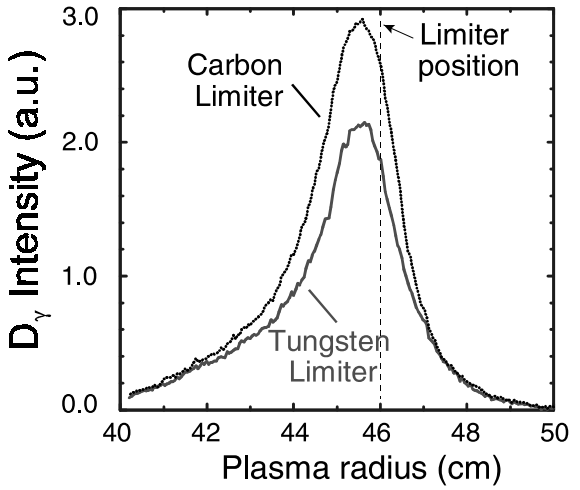

Fig. 4. Radial distributions of D_γ from tungsten and carbon limiters.

the D-flux is the same on carbon and tungsten surfaces, the integral of D_γ intensity at the carbon side is about 20–30% larger than at the tungsten surface. The particle reflection coefficients R_n for D on W and C are about 60% and 15% (angle $= 0°$, $T_e = 60$ eV, $T_i = 1.5 \times T_e$), respectively and the energy reflection coefficients R_e of the projectiles are about 37% and 5% [9]. The penetration depth λ of D atoms are characterized by e-folding length of the D_γ-emission into the plasma. We find that λ varies between $\approx$15 mm at the lowest densities and $\approx$10 mm at the highest densities [10]. From this a maximum velocity v of the released D atoms can be estimated according to $v = \lambda \times n_e \langle \sigma v \rangle_{ion} = 5 \times 10^3$ m/s which is much smaller than the velocity of reflected D particles ($\approx 1.4 \times 10^5$ m/s). These slow atoms are all ionized within the radial range of the observation volume from 40 to 50 cm. Due to the deeper penetration of the reflected particles, about 70% of these are ionized outside the observation volume. Thus the fraction of D_γ photons observed is given by $1 - R_n + R_n \times 0.3$. With the known values for R_n we obtain 60% and 90% for W and C, respectively (60%/90% = 1:1.5). This explains the main difference between the integral emission intensity of D_γ on W and C, which is 1.2–1.3. The remaining difference may be due to the fact that more D atoms leave the carbon surface in the form of D_2 compared to the W surface, which would decrease the number of D_γ photons per ionization events [11].

3.3. Power deposition

The heat flux to the limiter has been calculated by solving the time-dependent heat conduction equation. For simplicity, a one-dimensional heat flow in the material with infinite thickness is assumed as given by $\partial T/\partial t = 1/c\rho(\partial/\partial x)\lambda(\partial/\partial x)T$, where x is the direction perpendicular to the surface, and C, ρ, λ are the specific heat conductivity, density and thermal conductivity of the limiter material. The temperature dependencies of C and λ and the power loss due to the Planck radiation from the surface are taken into account. The surface temperature of the limiter was measured on one location by a pyrometer and a 2D pattern was obtained by an infrared camera.

Fig. 5 shows the heat flux as a function of the central-averaged electron density at the location of the pyrometer which is also the location of maximum power load onto the C- and W-limiter. On both sides the absorbed heat flux decreases with density: from 14 to 11 MW/m^2 on the carbon and from 11 to 8 MW/m^2 on the tungsten limiter. The absolute power deposition P_{abs} under identical plasma conditions is on carbon about 30% larger than on tungsten. The power P_{abs} transferred from plasma to the material surface can be written as [12]

$$P_{abs} = \Gamma\left[\left(2\frac{T_i}{T_e} - e\Phi_f/kT_e + (\approx)1/2\right)(1 - R_e) + 2\right]kT_e + S + (1 - R_n)E_r, \quad (1)$$

where Γ is the electron and ion flux density to the surface, T_e and T_i the electron and ion temperatures, R_e and R_n the energy and particle reflection coefficients, $e\Phi_f$ the sheath potential, S the ionization potential for hydrogen and E_r is the recombination energy of hydrogen atoms. With increasing density, the edge electron temperature decreases from 90 to 30 eV and the energy reflection coefficients R_e increase from 0.37 to 0.41 for D on W and from 0.05 to 0.07 for D on C [9]. Under the assumption angle $= 0°$, $e\Phi_f/kT_e = 3$ and $T_i/T_e = 1.5$ [13] the ratio P^C_{abs}/P^W_{abs} can be calculated from (1). The ratio varies between 1.34 for $T_e = 90$ eV ($\bar{n}_e = 2.2 \times 10^{19}$ m^{-3}) and 1.38 for $T_e = 30$ eV ($\bar{n}_e = 6 \times 10^{19}$ m^{-3}) and is in good agreement with the measured ratio of heat fluxes (see

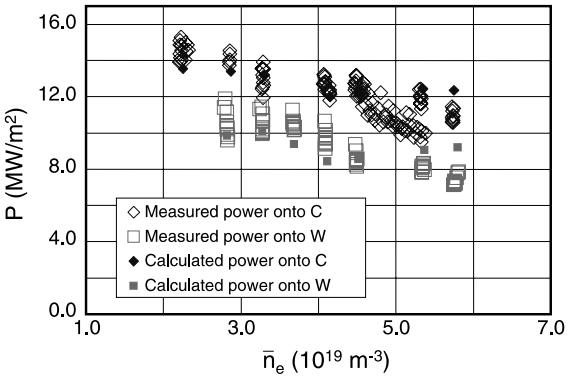

Fig. 5. Density dependence of the absorbed heat flux onto C- and W-limiters.

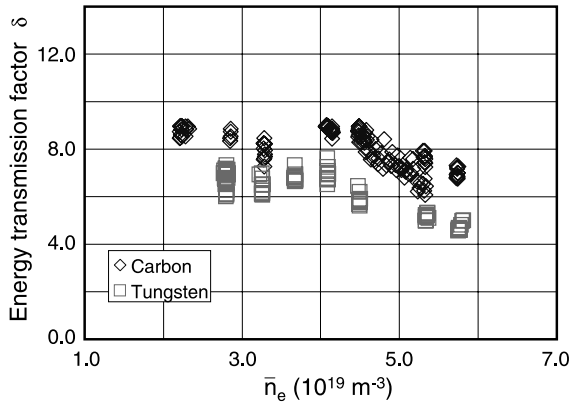

Fig. 6. The sheath energy transmission factor δ as a function of the electron density $\bar{n}_e$.

Fig. 5). Fig. 5 also shows the absorbed power calculated with (1). One sees that the agreement between measured and calculated absorbed power is very good.

Fig. 6 shows the evaluated sheath energy transmission factor, δ, as a function of the electron density $\bar{n}_e$ for carbon and tungsten. This factor was estimated from the relation $\delta = P_{abs}/\Gamma T_e \cos\alpha$, where P_{abs} is the measured deposited power on the carbon limiter, α the local angle between the surface and the magnetic field, and $\Gamma = 0.5 n_e c_s$ is the particle flux per unit area with c_s the ion acoustic velocity. Similar as for absorbed power, the measured factor δ is for both surfaces different: on the carbon side the factor is about 30% larger. The energy sheath transmission factor calculated from (1) decreases with increasing electron density and varies between 8.2 and 8.0 for graphite and between 6.1 and 5.8 for tungsten surface and is in good agreement with the measured factor δ as shown in the Fig. 6.

4. Conclusions

For a direct comparison of the impurity production, recycling and power deposition at carbon and tungsten surfaces, a C–W twin test limiter, half made of tungsten and another half made of carbon, was inserted into the edge plasma of TEXTOR-94. The release and recycling of impurities and hydrogen (W, C, O, D) from the two different surfaces (C and W) is examined spectroscopically for identical conditions. Although the D-flux is the same on carbon and tungsten surface, the intensity of the D_γ-line is about 20–30% larger on carbon, which is explained by the different hydrogen reflection properties and a different branching ratio of hydrogen release as atom or molecule. A post-mortem analysis showed no carbon layer ($<10^{15}$ C/cm^2) in the erosion region of the tungsten limiter. However, a carbon flux is observed on both sides, where the maximum intensity of the CII flux from the carbon surface is only $\approx$20% larger than that from the tungsten surface. This demonstrates clearly that the majority of the carbon release from both surfaces is from recycling of carbon impurities in the plasma edge and that only a small part of the detected carbon ($\approx$10%) is due to net-erosion from the bulk graphite limiter. The amount of carbon, which is released in the form of hydrocarbons from the tungsten surface is negligible compared to the graphite surface. The measured CII profiles can be well described by the ERO-TEXTOR code. The heat depositions on both sides under the same plasma conditions are different; on the carbon surface the absorbed power is about 30% larger. This can be explained by the different energy reflection coefficients of hydrogen. The heat deposition on the C- and W-limiters decrease both with density.

References

[1] T. Tanabe, N. Noda, H. Nakamura, J. Nucl. Mater. 196–198 (1992) 11.
[2] V. Philipps, A. Pospieszczyk, A. Huber et al., J. Nucl. Mater. 258–263 (1998) 858.
[3] B. Schweer, G. Mank, A. Pospieszczyk et al., J. Nucl. Mater. 196–198 (1992) 174.
[4] A. Kirschner, V. Philipps, J. Winter, U. Kögler, Nucl. Fus. 40 (2000) 989.
[5] W. Lotz, Z. Physik 216 (1967) 2412.
[6] H. Toyoda, H. Kojima, H. Sugai, Appl. Phys. Lett. 54 (1989) 1507.
[7] M. Rubel, V. Philipps, A. Huber, T. Tanabe, Phys. Scr. T 81 (1999) 61.
[8] J. Steinbrink, U. Wenzel, W. Bohmeyer et al., in: Proceedings of the 24th EPS Conference on Controlled Fusion and Plasma Physics, Part IV, vol. 21A, Berchtesgaden, Germany, 1997, p. 1809.
[9] W. Eckstein, Sputtering, reflection and range values for plasma edge codes, Max-Planck-Institut für Plasmaphysik, Report-IPP 9/117, 1998.
[10] A. Huber, V. Philipps, A. Pospieszczyk et al., in: Proceedings of the 26th EPS Conference on Controlled Fusion and Plasma Physics, vol. 23J, Maastricht, Netherlands, ECA, 1999, p. 685.
[11] A. Pospieszczyk, Ph. Mertens, G. Sergienko et al., J. Nucl. Mater. 266–269 (1999) 138.
[12] P.C. Stangeby, The plasma sheath, in: R. Langley, J. Bohdansky, W. Eckstein, P. Mioduszewski, J. Roth, E. Taglauer, E. Thomas, H. Verbeek, K. Wilson (Eds.), Data Compendium for Plasma-Surface Interactions (special issue), IAEA, Vienna, Nucl. Fus. (1984) 93.
[13] A. Huber, A. Pospieszczyk, B. Unterberg et al., Plasma Phys. Control. Fus. 42 (2000) 569.